



# Investigation on Thermally Induced Spin Crossover in Fe (Phen) Molecules

Hayder Fahim<sup>1,2#</sup>, Hashim Jabbar<sup>1\*</sup>, Adil A. Al-Fregi<sup>1@</sup>

<sup>1</sup>University of Basrah, College of Science, Iraq/Basrah

<sup>2</sup>Kerbala University, College of Education for Pure Science, Iraq/kerbala

(Received: 04 August 2023

Revised: 12 September

Accepted: 06 October)

## KEYWORDS

spin crossover,  
coordinating ligand,  
high spin (HS) state,  
low spin (LS) state

## ABSTRACT:

This study focuses on investigating the impact of an external stimuli of temperature on spin crossover in coordination complexes composed of  $Fe(phen)_2(NCS)_2$ , where (phen) stands for 1,10-phenanthroline). Based on the structure of the coordinating ligand sphere, these complexes are capable of thermally induced spin transitions or (SCO: spin crossover) from a low-spin (LS) to a high-spin (HS) state. We have shown that this unique effect lowers the equilibrium temperature and increases the HS fraction at lower temperatures. Due to both short- and long-range molecular interactions, the crossover proceeds as a function of temperature, resulting in a first-order phase transition. The complex  $Fe(phen)_2(NCS)_2$  contains Fe(II) surrounded by six nitrogen atoms. Our aim is to explore the thermodynamics of spin crossover systems to simulate bistable behaviors and multistep conversions observed in first-order spin transitions. These transitions are driven by the cooperative interactions of SCO molecules within the crystal structure, leading to the observed bistability.

## 1. Introduction:

Transition-metal ion complexes can undergo a fascinating phenomenon called spin transition (ST) or spin crossover (SCO) under specific conditions such as temperature, pressure, light, electric or magnetic fields [1]. During spin transition, the spin state of the central metal ion changes, leading to significant alterations in the electronic configuration and physical/chemical properties of the complex molecule. Notably, SCO compounds exhibit changes in magnetic properties and color, making them highly desirable for various spintronic applications such as switches [2], display and memory devices [3], sensors [4], electrical and electroluminescent devices [5], and MRI contrast agents [6]. The concept of "magnetic isomerism" or the initial thermal spin state shift (spin transition, spin crossover) was first introduced more than eighty years ago by Cambi, Szegö, and Cagnasso [7]. In their study, they investigated the magnetic characteristics of a series of

iron(III) dithiocarbamate complexes by varying the substituents on the dithiocarbamate ligand. Through magnetic susceptibility measurements, they observed that some samples displayed magnetic moments equivalent to five unpaired electrons, indicating a high-spin state (HS), while others exhibited magnetic moments corresponding to only one unpaired electron, indicating a low-spin state (LS) at room temperature.

Interestingly, a third category of compounds has been discovered, exhibiting unique magnetic behavior where they display high-spin (HS) characteristics at room temperature but undergo a gradual transition to low-spin (LS) behavior as they are cooled [8], [9]. Subsequently, extensive studies were conducted on various iron(III) spin crossover (SCO) complexes such as  $\{FeO_6\}$ ,  $\{FeO_3 S_3\}$ ,  $\{FeS_6\}$ ,  $\{FeN_2 O_2 S_2\}$ ,  $\{FeN_3 O_3\}$ , or  $\{FeN_6\}$ . More than three decades after the initial discovery of thermal spin transition, the first iron(II) coordinated complex,  $\{Fe(phen)_2(NCS)_2\}$  (phen =



1,10 – phenanthroline), was reported to undergo a thermally induced spin transition between the HS and LS states at 175 K [10], [11]. Since then, numerous iron(II) SCO compounds have been reported [12], [13], and to a lesser extent, some coordination compounds of 3d transition metals like cobalt(II) [14], as well as cobalt(III), chromium(II), manganese(II), manganese(III), and nickel [15], [16]. However, the occurrence of thermal spin transition in coordination compounds of the 4d and 5d transition metal series is rare, which can be explained by ligand field theory [17].

In 2013, Philipp Gütlich and colleagues conducted a comprehensive study on the fundamental aspects of spin crossover in iron coordination compounds. They explored various aspects, including electronic structure, thermodynamics, and recent advancements in the field. The research highlighted the potential applications of spin crossover compounds in optical switching devices, memory devices, and spintronic components. Additionally, the article addressed the challenges and opportunities that lie ahead for the future development of spin crossover materials [18].

In 2015, Samir F. Matar and colleagues published a paper discussing the application of computational methods in studying spin crossover (SCO) complexes. The research focused on investigating the LS/HS switching phenomenon that occurs in response to small variations in temperature, pressure, or light, including the Light-Induced Excited Spin-State Trapping (LIESST) process. The study showcased the capabilities of computational methods in examining the properties and behavior of SCO complexes at various levels, ranging from isolated molecules to extended solids. This research highlights the potential of computational approaches in advancing the understanding of SCO materials [19].

In 2017, Lars Kreutzburg and collaborators conducted a computational study on the spin crossover complex  $[\text{Fe}(\text{phen})_2(\text{NCS})_2]$ . Their research involved calculating the enthalpies of all 16 spin configurations and determining the spin couplings using an Ising-like model. Monte Carlo simulations were then employed to estimate the interaction parameter  $G$ , which characterizes

the cooperativity of the spin transition. The study demonstrated that the estimated value of  $G$  aligned with experimental findings, indicating the potential of this approach in predicting the impact of modifications to spin crossover complexes on the spin transition. This work offers valuable insights into the understanding and design of spin crossover systems [20].

In 2019, Jordi Cirera and Eliseo Ruiz conducted a comprehensive review of computational methods employed for determining thermochemical properties and transition temperatures in spin-crossover (SCO) systems. The study focused on elucidating trends observed in various families of SCO molecules and investigating the influence of chemical modifications on the ligand-field surrounding the metal center. The findings of this research contribute to the understanding of SCO systems and offer valuable insights for the design of new SCO systems with tailored properties [21].

In 2020, Saho Kajikawa and Azusa Muraoka conducted a study focusing on the application of density functional theory (DFT) calculations to identify a functional that effectively captures the energy gap, electronic state, and infrared spectra of a Fe(II) spin-crossover complex. The selection of an appropriate functional was guided by comparing the calculated enthalpy difference with experimental values. The study also revealed significant structural variations around the Fe atom upon optimization, and the vibrational intensity was found to be influenced by the spin state of the complex [22].

In 2022, Yachao Zhang conducted a study investigating the influence of substrates on the thermal spin crossover (SCO) behavior of  $[\text{Fe}(\text{phen})_2(\text{NCS})_2]$  when deposited on metallic surfaces and 2D materials. Utilizing first-principles calculations, the study found that the SCO phenomenon is maintained on hexagonal boron nitride and molybdenum disulfide, whereas low-spin states dominate on metal surfaces. The spin transition temperature was observed to be highly dependent on the surface environment, with the effect attributed to modifications in electronic structures and molecular vibrations upon adsorption [23].



## 2. The model

### 2.1 Entropy driven spin-crossover

The enthalpy and entropy variations can be dissected into different components. The change in enthalpy ( $\Delta H$ ) consists of two distinct parts: the temperature-independent electronic contribution denoted as  $\Delta H_{el}$  and the vibrational contribution represented as  $\Delta H_{vib}$ . Likewise, the change in entropy ( $\Delta S$ ) can be decomposed into various contributions accounting for statistical disorder.

$$\Delta S = \Delta S_{el} + \Delta S_{vib} + \Delta S_{trans} + \Delta S_{rot} \dots \dots (1)$$

The last two components,  $\Delta S_{trans}$ , and  $\Delta S_{rot}$ , pertain to the entropy changes associated with translation and rotation, respectively, and are generally disregarded in the solid state. The first component,  $\Delta S_{el} = \Delta S_{orb} + \Delta S_{spin}$ , accounts for the electronic entropy variation and originates from the disparity in degeneracy (related to orbital and spin momenta) between the high-spin (HS) and low-spin (LS) electronic states:

$$\Delta S_{orb} = R \left[ \ln (2L + 1)_{HS} - \ln (2L + 1)_{LS} \right] \dots \dots (2)$$

and

$$\Delta S_{spin} = R \left[ \ln (2S + 1)_{HS} - \ln (2S + 1)_{LS} \right] \dots \dots (3)$$

The perfect gas constant  $R$ , as well as the total orbital ( $L$ ) and total spin ( $S$ ) momenta of the spin state, play a significant role in the thermodynamics of the system. The contribution of spin degeneracy emerges from the alteration in state degeneracy as the system undergoes a transition between low-spin (LS) to high-spin (HS) and vice versa.

For an ideal spin-crossover (SCO) Fe(II) complex with perfect octahedral symmetry, we observe  $\Delta S_s = R \ln (5) = 13.38 \text{ J mol}^{-1} \text{ K}^{-1}$  and  $\Delta S_{orb} = R \ln (3) = 9.13 \text{ J mol}^{-1} \text{ K}^{-1}$ . However, in practical scenarios, there is typically no orbital degeneracy due to Jahn-Teller distortion, resulting in the blocking of orbital momentum ( $L$ ) leading to  $L = 0$ . Hence, the contribution of the orbital momentum to the entropy change is commonly disregarded.

Therefore, the primary contribution to  $\Delta S_{el}$  is attributed to the change in entropy caused by spin degeneracy, and this can be expressed as follows:

$$\Delta S_{el} = R \left[ \ln (2S + 1)_{HS} - \ln (2S + 1)_{LS} \right] \dots \dots (4)$$

Thus, for Fe(II)-centered spin-crossover molecules in octahedral geometry, with  $s = 2$  representing the high-spin (HS) state and  $s = 0$  representing the low-spin (LS) state, the change in electronic entropy,  $\Delta S_{el}$ , is given by  $\Delta S_{el} = R \ln (5/1) = 13.38 \text{ J mol}^{-1} \text{ K}^{-1}$  [24]. It's important to note that temperature does not influence the electronic entropy, favoring the HS state.

The second term,  $S_{vib}$  (vibrational entropy), accounts for the variation in intramolecular modes between the HS and LS states in the case of isolated molecules. When dealing with solid states, the contribution from intermolecular vibrations must also be considered, although it is often regarded as less significant than intramolecular vibrations. However, it can be challenging to distinguish between intermolecular and intramolecular vibrational contributions as they are typically interconnected. The vibrational entropy can be expressed as described in Ref. [25] for further detailed analysis:

$$S_{vib}(T) = R \sum_{\lambda} \left( -\ln \left[ 1 - e^{-h\nu_{\lambda}/k_B T} \right] + \frac{h\nu_{\lambda}}{k_B T} \frac{1}{\exp(h\nu_{\lambda}/k_B T)} \right) \dots \dots (5)$$

Where the summation  $\sum_{\lambda}$  runs over all vibration modes. A convenient assumption is the low-frequency approximation ( $h\nu \ll k_B T$ ), in which case Equation 5 simplifies to:

$$S_{vib} = -R \sum_{\lambda} \left( \ln \frac{h\nu_{\lambda}}{k_B T} \right) \dots \dots (6)$$

Indeed, the vibrational entropy change can be described by considering the entropy of an ensemble of harmonic oscillators.

$$\Delta S_{vib} = S_{vib}^{HS} - S_{vib}^{LS} = R \sum_{\lambda=1}^{15} \ln \left( \frac{\nu_{\lambda}^{LS}}{\nu_{\lambda}^{HS}} \right) = 15R \ln \left( \left\langle \frac{\nu_{\lambda}^{LS}}{\nu_{\lambda}^{HS}} \right\rangle \right) \dots \dots (7)$$

Considering a perfect octahedron with  $\lambda=15$  molecular vibrational modes and adopting the ratio  $\langle \nu_{\lambda}^{LS} \rangle / \langle \nu_{\lambda}^{HS} \rangle = 1.3$ , we find that  $\Delta S_{vib}$  is calculated to be  $32.7 \text{ J mol}^{-1} \text{ K}^{-1}$ , which is consistent with experimental measurements [26].

During spin-crossover, the lengths of metal-ligand bonds change, leading to alterations in stretching frequencies. These modifications in phonon modes give rise to the vibrational component of the overall entropy change. In the majority of spin-crossover complexes, the



vibrational contribution plays a dominant role in the total entropy change [24].

On the other hand, the rotational degree of freedom of the complexes makes a minimal contribution to the entropy change [27]. It can be calculated semi-classically using the equation:

$$\Delta S_{\text{rot}} = R \ln \left( Z_{\text{rot}} + \frac{3}{2} \right) \dots \dots (8)$$

where  $Z_{\text{rot}} = \left( \frac{\sqrt{2}}{\pi} \right)^3 \left( \frac{\sqrt{\pi}}{\sigma} \right) (k_B T)^{3/2} (J_1 J_2 J_3)^{1/2}$ , with  $J_i$  being the moments of inertia and  $\sigma$  as the symmetry number. The value of  $\sigma$  is 2 for  $C_2$  symmetry and 1 for  $C_1$  symmetry. Typically, the entropy change due to rotation is in the order of  $1 J \cdot \text{mol}^{-1} \cdot \text{K}^{-1}$  [24].

This implies that the majority of the entropy change in thermal spin-crossover is mainly contributed by vibrational effects, with electronic effects playing a lesser role. In a spin-crossover transition, both  $\Delta H$  and  $\Delta S$  are positive [27], [28]. The variation in Gibbs free energy can be reformulated as:

$$\Delta G(T, p) = \Delta H \left( 1 - \frac{T \Delta S}{\Delta H} \right) = \Delta H \left( 1 - \frac{T}{T_{1/2}} \right) \dots \dots \dots (9)$$

In this situation, we use the temperature  $T_{1/2} = \frac{\Delta H}{\Delta S}$ , leading to  $\Delta G = 0$ . At the  $T_{1/2}$  temperature, the Gibbs free energy of both spin states becomes identical, resulting in an equal likelihood of both high-spin and low-spin states being occupied. This  $T_{1/2}$  value is commonly referred to as the half-transition temperature and signifies the point where the system is evenly balanced between the high-spin and low-spin states.

This temperature is referred to as the transition temperature. Fig.3 illustrates the adiabatic potentials of the high-spin (HS) and low-spin (LS) states of a Fe(II) spin-crossover complex, plotted against the totally symmetric metal-ligand stretching distance ( $r(\text{Fe-L})$ ).

Thermal spin-crossover is governed by the zero-point energy difference ( $\Delta E^0_{\text{vib}}$ ,  $\Delta G$ ) between the high-spin (HS) and low-spin (LS) states, which needs to be in the order of thermal energy  $k_B T$ . At  $T = 0\text{K}$ ,  $\Delta G = \Delta H$ , making the LS state thermodynamically favored (as  $\Delta H > 0$ ). Generally, at temperatures below  $T_{1/2}$ , the LS state is preferred (since  $\Delta G > 0$ ), while at temperatures above  $T_{1/2}$ , the HS state becomes favored (due to  $\Delta G < 0$ ). During thermal spin-crossover, the metal-ligand bond

length undergoes an abrupt change, resulting in a shift in the ligand field strength. The ligand field strength ratio between the LS and HS states is given by Eq.  $\left[ \frac{10Dq^{\text{LS}}}{10Dq^{\text{HS}}} = \left( \frac{r_{\text{HS}}}{r_{\text{LS}}} \right)^n \right]$ , where  $n$  lies between 5 and 6.

Because  $r_{\text{HS}}$  is greater than  $r_{\text{LS}}$ , the ligand field strength sharply decreases during the transition from LS to HS. The driving force behind this transition is the change in entropy ( $\Delta S$ ), which affects the value of  $\Delta G$ . As a result, thermal spin-crossover is often referred to as an entropy-driven phenomenon.

## 2.2 Effect of Metal-Ligand Bond Distance

The shift from a high spin to a low spin state occurs through the transfer of one or two electrons (depending on the d-electron configuration) from the higher energy  $e_g$  orbitals ( $d_{x^2-y^2}$  and  $d_{z^2}$ ) to the lower energy  $t_{2g}$  orbitals ( $d_{xy}$ ,  $d_{xz}$ , and  $d_{yz}$ ). The  $e_g$  orbitals directly face the approaching ligands along the coordinate axis, while the  $t_{2g}$  orbitals are situated between the ligand-induced point charges. This leads to increased electron repulsion between the metal's  $e_g$  orbitals and the ligand's electron pair, causing the  $e_g$  orbitals to have higher energy compared to the  $t_{2g}$  orbitals [29].

## 2.3 Thermodynamics of spin crossover systems

The system's spin state is determined by its free energy, expressed as  $G = H - TS$ , where  $H$  is the enthalpy,  $T$  is the temperature, and  $S$  is the entropy. When considering a group of Na molecules, the free energy difference between the high-spin (HS) and low-spin (LS) states can be calculated as  $\Delta G = G_{\text{HS}} - G_{\text{LS}} = \Delta H - T\Delta S$  at a constant pressure. The state with the lowest free energy is considered to be the thermodynamically stable phase. The enthalpy term,  $H$ , is mainly influenced by  $H_{\text{en}}$ , which accounts for the variation in zero-point energy between the HS and LS states due to changes in bond length and ligand field. This energy difference is significant and plays a crucial role in determining the system's spin state [14], [28].

$$\Delta H = H_{\text{enHS}} - H_{\text{enLS}} \dots \dots \dots (10)$$

The LS state has a narrower potential well compared to the HS state due to higher metal-ligand bond oscillation frequencies [30]. Figure 5(a) provides a visual representation of this concept.

The entropy term,  $\Delta S$ , consists mainly of two contributions: the electronic contribution ( $\Delta S_{\text{el}}$ ) and the



vibration contribution ( $\Delta S_{\text{vib}}$ ), according to research conducted at the University of California, Berkeley. The electronic contribution is determined by the ratio of degeneracies between the two states and can be mathematically described by the following equation:

$$\Delta S_{\text{el}} = N \times k_B \times \ln \left[ \frac{\Omega_{\text{HS}}}{\Omega_{\text{LS}}} \right] \dots \dots \dots (11)$$

In the equation,  $\Omega_{\text{HS}}$  and  $\Omega_{\text{LS}}$  represent the degeneracies of the high-spin (HS) and low-spin (LS) states, respectively. For Fe(II), the  $\Omega_{\text{HS}}/\Omega_{\text{LS}} = 2S + 1 = 5$  [31]. The electronic contribution to entropy,  $\Delta S_{\text{el}} = 13,38 \text{ J} \cdot \text{K}^{-1} \cdot \text{mol}^{-1} > 0$ . This factor accounts for a small portion of the overall entropy change [53,54,58-60]. It's important to note that Jahn-Teller distortions, which increase orbital degeneracies, do not contribute to a change in entropy [32].

The vibrational modes of the molecules, denoted as  $S_{\text{vib}}$ , contribute significantly to the entropy change. These modes involve stretching, bending, and deformations of the molecules and networks. The difference in vibrational entropy,  $\Delta S_{\text{vib}} = S_{\text{vibHS}} - S_{\text{vibLS}} > 0$  because the density of phonons and vibrational disorder is more significant in the high-spin (HS) state where the coordination sphere is enlarged, compared to the low-spin (LS) state where it is decreased.

As a result, there exists a temperature, denoted as  $T_{\text{transition}}$ , at which equilibrium is reached with  $\Delta H/\Delta S > 0$  and  $\Delta G = 0$ . Above this temperature, the thermodynamically stable state is HS ( $\Delta G < 0$ ), while below this temperature, the stable state is LS ( $\Delta G > 0$ ). At the transition temperature, also referred to as  $T_{1/2}$  in

the literature, 50% of the sample's molecules are in the HS state [33].

Now, let's consider the high-spin fraction of HS molecules in the sample, denoted as  $n_{\text{HS}}$ , which varies with temperature. For a system with  $N$  molecules, there are two possible configurations: HS with a ratio of  $n_{\text{HS}}$  and LS with a ratio of  $(1 - n_{\text{HS}})$ . The system's free energy can be expressed as follows:

$$G = n_{\text{HS}}G_{\text{HS}} + (1 - n_{\text{HS}})G_{\text{LS}} - TS_{\text{mix}} \dots \dots \dots (12)$$

The mixing entropy, denoted as  $S_{\text{mix}}$ , represents the entropy contribution when HS and LS molecules are perfectly mixed together. It can be mathematically expressed as follows:

$$S_{\text{mix}} = -R[n_{\text{HS}}\ln(n_{\text{HS}}) + (1 - n_{\text{HS}})\ln(1 - n_{\text{HS}})] \dots \dots (13)$$

### 3. Results and Discussion

Two significant conclusions can be drawn from these findings. Firstly, the high-spin (HS) state exhibits greater vibrational entropy, making it more favorable at elevated temperatures. Consequently, the entropy change in thermal spin-crossover is primarily attributed to the vibrational contribution, with the electronic contribution playing a comparatively smaller role. Generally, the entropy variation  $\Delta S$  falls within the range of 40 to 80  $\text{J} \cdot \text{K}^{-1} \cdot \text{mol}^{-1}$ , as opposed to  $\Delta S_{\text{el}}$  which equals 13.38  $\text{J} \cdot \text{K}^{-1} \cdot \text{mol}^{-1}$ . These thermodynamic properties can be determined through calorimetric measurements [27], (as shown in Fig.1), while vibrational properties can be assessed using Raman and infrared spectroscopies [34].

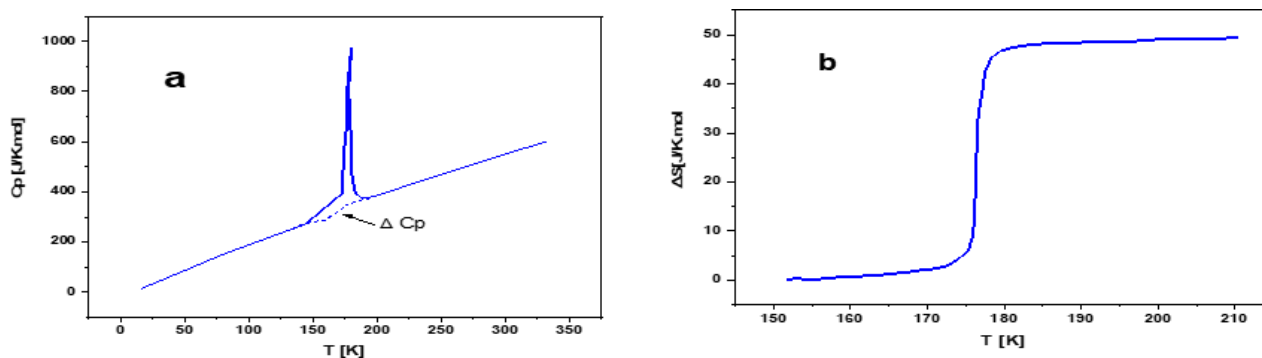


**Figure 1:** (a) The heat capacity of the  $[\text{Fe}(\text{phen})_2(\text{NCS})_2]$  crystal changes with temperature. The symbol  $\Delta C_p$  represents the abrupt change linked to the spin transition. (b), the graph shows the temperature-dependent variation of entropy for the same compound [27].



If we take into account  $N$  noninteracting molecules, out of which  $N_{\text{HS}}$  are in the high-spin (HS) state, we can define the HS fraction as  $n_{\text{HS}} = N_{\text{HS}} / N$ . However, it should be noted that this HS fraction is mistakenly referred to as the order parameter of the spin transition. The Gibbs energy of a spin-crossover (SCO) system can be represented as follows:

$$G = n_{\text{HS}} G_{\text{HS}} + (1 - n_{\text{HS}}) G_{\text{LS}} - TS_{\text{mix}} \dots\dots (14)$$

The considerable number of ways  $N_{\text{HS}}$  molecules can be distributed among  $N$  molecules in the high-spin (HS) state leads to the mixing entropy, which represents a loss of statistical information in the system. The expression for mixing entropy can be formulated in the thermodynamic limit.

$$S_{\text{mix}} = -k_{\text{B}} N [n_{\text{HS}} \ln(n_{\text{HS}}) + (1 - n_{\text{HS}}) \ln(1 - n_{\text{HS}})] \dots\dots (15)$$

The equilibrium condition can be expressed as:

$$\left( \frac{\partial G}{\partial n_{\text{HS}}} \right)_{T,p} = 0 \dots\dots (16)$$

By following the thermal evolution of the HS fraction (as shown in Fig. 2), the temperature ( $T$ ) can be determined using the formula:

$$T = \frac{\Delta H}{R \ln \left( \frac{1 - n_{\text{HS}}}{n_{\text{HS}}} \right) + \Delta S} \dots\dots (17)$$

Where  $\Delta S$  is calculated as  $\Delta s = R \ln \Omega$ , with  $\Omega$  representing the effective degeneracy. By substituting this value of  $\Delta S$ , expression (17) can be rephrased as  $\ln \frac{n_{\text{HS}}}{1 - n_{\text{HS}}} = \Omega e^{-\Delta H/RT}$ .

As a result of the equilibrium condition, we obtain the Arrhenius law, expressed as:

$$\ln \frac{n_{\text{HS}}}{1 - n_{\text{HS}}} = \ln \Omega - \Delta H/RT \dots\dots (18)$$

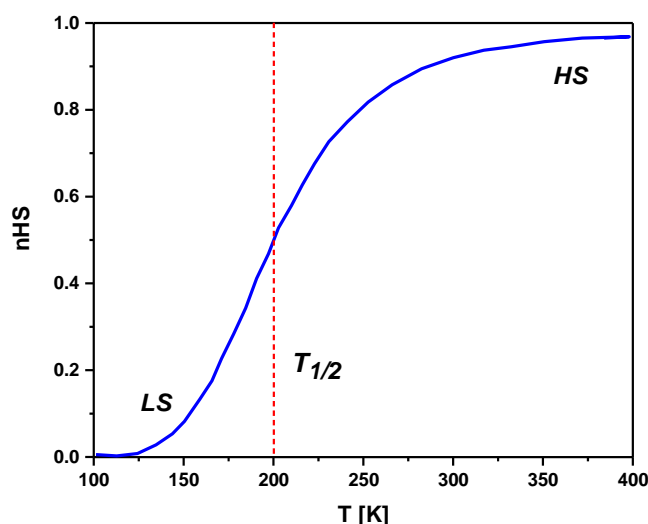


**Figure 2:** The thermal variation of the HS fraction,  $n_{\text{HS}}$  (shown as the blue line), for noninteracting spin-crossover (SCO) molecules. The temperature at which the HS fraction reaches half of its maximum value is denoted as  $T_{1/2}$ .

In noninteracting spin-crossover (SCO) molecules, a consistent transfer of spins from the low-spin (LS) to the high-spin (HS) state is only achievable by increasing the temperature. The emission or absorption of latent heat, which arises solely from the interactions between

SCO molecules, is directly linked to the occurrence of rapid first-order transitions characterized by bi-stability phenomena.

Consequently, an  $e_g \rightarrow t_{2g}$  transition often results in a reduction of the metal-ligand bond distance ( $R$ ). As



the spin crossover ( $\Delta$ ) is dependent on  $R$  ( $\Delta \propto 1/R^5$ ), this transition leads to an approximately 10-20% increase in  $\Delta$ . Figure 3 illustrates potential energy curves for the high spin and low spin complexes. In the low-spin state, the minimum energy occurs at a smaller  $R$  value than in the

high spin state. Figure 3a and 3c represent the ground states for high spin and low spin, respectively, while Figure 3b shows the equilibrium situation, where the energies of both spin states are closely matched, resulting in a crossover effect.

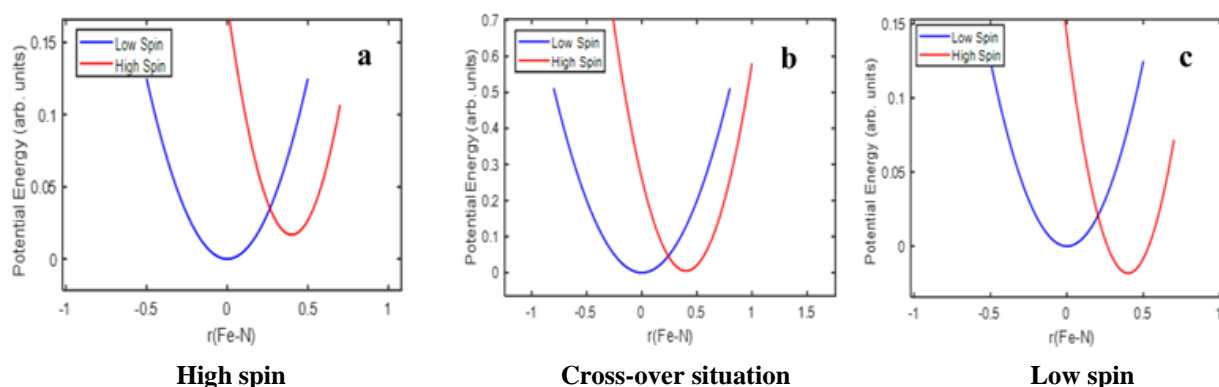


**Figure 3:** Potential energy curves of the LS and HS states of an octahedral SCO complex, (a) high spin complexes, (b) cross-over situation, and (c) low spin complexes.

The figure illustrates potential energy curves for coordination complexes with different electronic configurations and spin states. High spin complexes have weakly bound ligands and more unpaired electrons, while low spin complexes have strongly bound ligands and fewer unpaired electrons. The cross-over situation occurs when the energies of high spin and low spin states become equal, allowing for switching between configurations. These curves provide valuable information about the complexes' stability and behavior under varying conditions.

Figure 6 illustrates how two properties, the average Fe – N bond lengths (represented by orange circles) and the dihedral angle between ligand coordination planes (shown as blue triangles), vary with temperature in a single crystal of the [Fe(phen)] complex.

**Average Fe – N bond lengths (orange circles):** This data shows the average distances between the central iron (Fe) atom and the surrounding nitrogen (N) atoms in the ligands of the [Fe(phen)] complex. The values of these bond lengths are measured at different temperatures, and the orange circles represent the corresponding values.

**Dihedral angle between ligand coordination planes (blue triangles):** This data represents the angle between the planes formed by the ligands that coordinate around the central iron atom. The dihedral angle is measured at different temperatures, and the blue triangles indicate the values at each temperature point.

The x-axis in the graph represents the temperature, and the y-axis shows the respective values of the average Fe – N bond lengths (in Angstroms) and the dihedral angles (in degrees).

The crosses on the graph correspond to the structure of the [Fe(phen)] complex after it has been heated to 450 K, and the solvent molecule has been lost. This data point provides information about the complex's behavior at this specific temperature and condition.

Overall, the figure provides a visual representation of how the average Fe-N bond lengths and the dihedral angles between ligand coordination planes change with temperature in the [Fe(phen)] complex. This information is crucial for understanding the complex's structural characteristics and its response to changes in temperature.

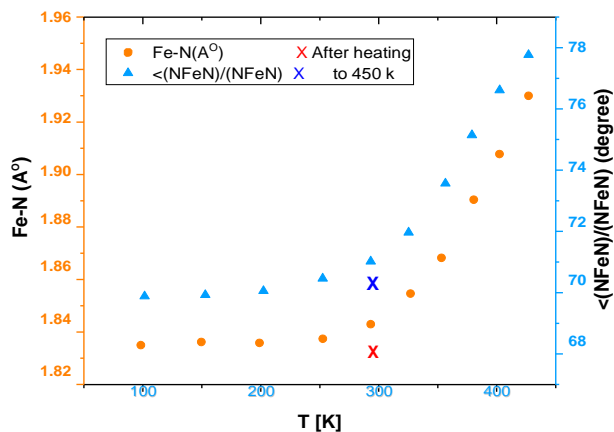


**Figure 4:** The average Fe – N bond lengths (represented by orange circles) and the dihedral angle between ligand coordination planes (shown as blue triangles) as the temperature varies in a single crystal of the  $[\text{Fe}(\text{phen})]$ . The crosses on the graph represent the structure after heating to 450 K and the loss of the solvent molecule.

We can determine the fraction of HS molecules at a given temperature by analyzing the condition of thermal equilibrium, where the derivative of Gibbs free energy with respect to the fraction of HS molecules

$$\left. \frac{\delta G}{\delta n_{\text{HS}}} \right|_T = 0,$$

$$n_{\text{HS}} = \frac{1}{1 + \exp\left(\frac{\Delta H - T\Delta S}{RT}\right)} \dots \dots \dots (19)$$

The theoretical values for the compound  $(\text{Fe}(\text{phen})_2(\text{NCS})_2)$  are presented in Figure 5, with enthalpy  $H = 8600 \text{ J} \cdot \text{mol}^{-1}$  and entropy  $S = 48,78 \text{ J} \cdot \text{K}^{-1} \cdot \text{mol}^{-1}$  [27].

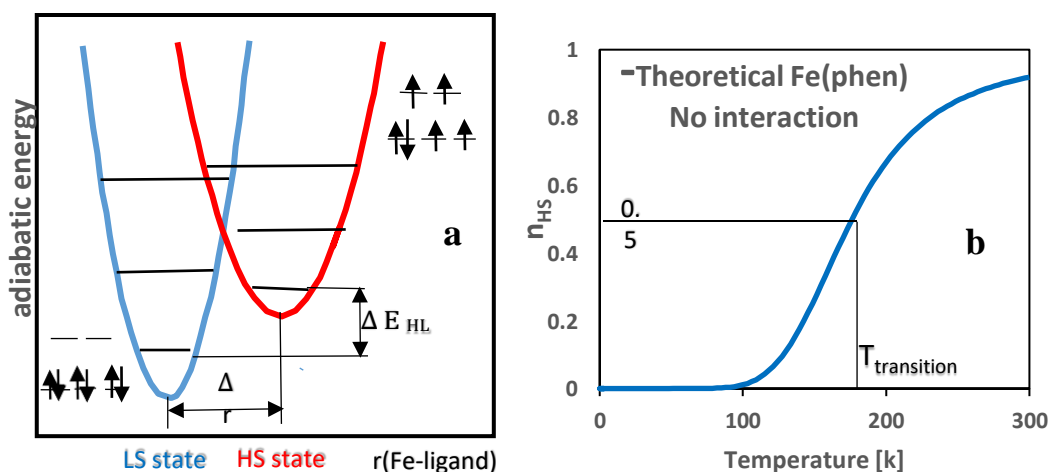


**Figure 5:** (a) The relationship between molecular system potential energy and metal-ligand bond length  $r_{\text{Fe-N}}$ , during a thermal spin transition. Panel (b) represents the spin transition using the equation 19 for  $\text{Fe}(\text{phen})_2(\text{NCS})_2$  values. The curve  $n_{\text{HS}}(T)$  in panel (b) demonstrates a smooth shape, indicating a gradual spin transition occurring over a wide temperature range.



It is important to highlight that the example illustrated in Figure 5b does not depict the typical behavior of  $n_{\text{HS}}$  (T) in most experimental scenarios. Smooth transitions as shown are only observed in weakly cooperative systems, such as diluted liquids or complexes with weak intermolecular interactions. In contrast, systems with strong intermolecular interactions often exhibit cooperative behavior, which can lead to abrupt transitions or hysteresis, contrary to common expectations [14], [35], [36].

The original thermodynamic model proposed by Slichter et al. in 1972 is just one of several available models, such as Ising-like, Sorai, Vibronic, or elastic models. However, for the purpose of comparison with existing literature and presenting results with a few key parameters, we will use the original form of the thermodynamic model [37].

Rao et al. conducted a study on the spin transition in Fe(phen) and found that a more generalized model, based on the Kimmermann model, provided a better description of the results compared to a domain model like the one proposed by Sorai et al. To account for the cooperative behavior of the molecules, they introduced a cooperative factor denoted as  $\Gamma$  into the Gibbs energy equation. This factor  $\Gamma$  is proportional to the product of the high-spin (HS) and low-spin (LS) fractions in the sample [38], [27], [39]. The parameter  $\Gamma$  can be considered as a term in a power series expansion of the Gibbs free energy (G) with respect to the variable  $n_{\text{HS}}$ , satisfying the condition  $(G/n_{\text{HS}})_{P, T} = 0$ . In this case,  $\Gamma$  is a phenomenological constant assumed to be

independent of temperature, without making any assumptions about the origin of cooperativity.

However, recent simulations by Kepenekian et al. suggest that electrostatic interactions in the structure, particularly in hysteretic complexes, are the primary source of  $\Gamma$ .  $\Gamma$  can be expressed as  $\Delta Q(\delta V_{\text{LS}} - \delta V_{\text{HS}})$ , where  $\Delta Q$  represents the change in charge on the Fe(II) ion, and  $(\delta V_{\text{LS}} - \delta V_{\text{HS}})$  is a term dependent on the fluctuation of polarization during the spin transition, which strongly depends on crystal stacking. Therefore, the equation describing the temperature-dependent evolution of the HS fraction can be written as:

$$T(n_{\text{HS}}) = \frac{\Delta H + \Gamma(1 - 2n_{\text{HS}})}{R \ln \left( \frac{1 - n_{\text{HS}}}{n_{\text{HS}}} \right) + \Delta S} \quad (20)$$

The shape of the curve representing the percentage of high-spin (HS) molecules as a function of temperature is determined by the relative values of  $\Delta H$ ,  $\Delta S$ , and  $\Gamma$ . Fig.6, based on the Fe(phen) scenario depicted in Fig.1, illustrates this relationship. The red curve corresponds to a value of  $\Gamma = 3000 \text{ J. mol}^{-1}$ , which is similar to the cooperative parameter  $J_2 = 3850 \text{ J. mol}^{-1}$  proposed by Rao et al. [40]. On the other hand, the blue curve corresponds to a value of  $\Gamma = 4000 \text{ J. mol}^{-1}$ . The blue curve exhibits a "forbidden" shape, indicating the presence of thermal hysteresis and bistability in the system, where two different HS percentages are observed at the same temperature. This observation aligns with the observed thermal hysteresis in the spin-crossover (SCO) sample.

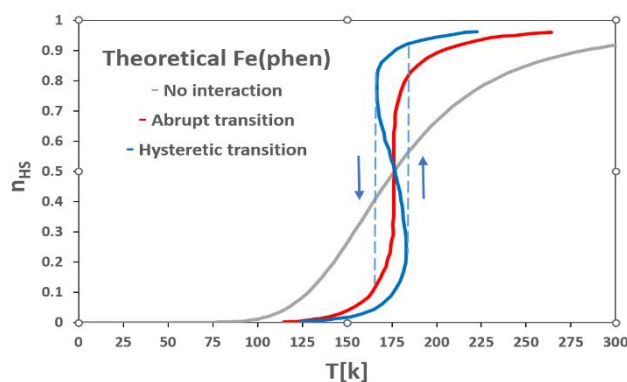


**Figure 6:** The variation of the computed HS proportions as a function of temperature using equation 20. The (grey) curve is plotted for the case where  $\Gamma = 0 \text{ J. mol}^{-1}$ , while the (red and blue) curves are plotted for  $\Gamma = 3000 \text{ J. mol}^{-1}$  and  $\Gamma = 4000 \text{ J. mol}^{-1}$ , respectively. The arrows show the direction of the temperature sweep, while the dashed lines indicate the actual thermal hysteresis observed in the blue curve.



The spin-crossover process can involve more than two spin states depending on the number of metal centers in the target molecule. As a result, the spin transition can take place in multiple stages. This has been studied in various research works.

#### 4. Conclusion.

This research centered on the thermal spin transition in coordination complexes, specifically focusing on  $[\text{Fe}(\text{phen})_2(\text{NCS})_2]$ . The study discovered that the high-spin state becomes more favorable as temperatures increase, primarily due to the rise in vibrational entropy. It emphasized the crucial role played by thermodynamic properties and cooperative interactions in governing spin-crossover behavior, leading to bistability.

By utilizing a thermodynamic approach and conducting experimental investigations with thermodynamic models, the study offered valuable insights into bistable behaviors and multistep conversions during first-order spin transitions. It identified the cooperative behavior among spin-crossover (SCO) molecules in the crystal packing as a key factor responsible for bistability.

The analysis of the  $\text{Fe}(\text{phen})$  spin transition with varying parameters of  $\Gamma$  using thermodynamic models and equation 20 yielded different computed proportions of high-spin (HS), as depicted in Figure 6. These findings significantly advance our comprehension of spin-crossover phenomena and the underlying thermodynamic properties. Consequently, this research holds the potential to influence the development of molecular switches and data storage technologies.

#### References:

- [1] P. Gütllich and H. A. Goodwin, "Spin Crossover—An Overall Perspective," vol. 1, pp. 1–47, 2012, doi: 10.1007/b13527.
- [2] K. Senthil Kumar and M. Ruben, "Emerging trends in spin crossover (SCO) based functional materials and devices," *Coord. Chem. Rev.*, vol. 346, pp. 176–205, 2017, doi: 10.1016/j.ccr.2017.03.024.
- [3] O. Kahn and C. J. Martinez, "Spin-transition polymers: From molecular materials toward memory devices," *Science* (80-. ), vol. 279, no. 5347, pp. 44–48, 1998, doi: 10.1126/science.279.5347.44.
- [4] J. Park et al., "Soft, smart contact lenses with integrations of wireless circuits, glucose sensors, and displays," *Sci. Adv.*, vol. 4, no. 1, pp. 1–12, 2018, doi: 10.1126/sciadv.aap9841.
- [5] S. Song, H. Shim, S. K. Lim, and S. M. Jeong, "Patternable and Widely Colour-Tunable Elastomer-Based Electroluminescent Devices," *Sci. Rep.*, vol. 8, no. 1, pp. 1–10, 2018, doi: 10.1038/s41598-018-21726-x.
- [6] A. Datta and K. N. Raymond, "Gd-hydroxypyridinone (HOPO)-based high-relaxivity magnetic resonance imaging (MRI) contrast agents," *Acc. Chem. Res.*, vol. 42, no. 7, pp. 938–947, 2009, doi: 10.1021/ar800250h.
- [7] P. Gütllich and J. Jung, "Thermal and optical switching of iron(II) compounds," *J. Mol. Struct.*, vol. 347, pp. 21–38, 1995, doi: 10.1016/0022-2860(95)08534-3.
- [8] L. Cambi and L. Szegö, "Über die magnetische Suszeptibilität der komplexen Verbindungen," *Berichte der Dtsch. Chem. Gesellschaft (A B Ser.)*, vol. 64, no. 10, pp. 2591–2598, 1931, doi: 10.1002/cber.19310641002.
- [9] L. Cambi and L. Malatesta, "Magnetismus und Polymorphie innerer Komplexsalze: Eisensalze der Dithiocarbamidsäuren," *Berichte der Dtsch. Chem. Gesellschaft (A B Ser.)*, vol. 70, no. 10, pp. 2067–2078, 1937, doi: 10.1002/cber.19370701006.
- [10] K. S. Murray, "Advances in polynuclear iron(II), iron(III) and cobalt(II) spin-crossover compounds," *Eur. J. Inorg. Chem.*, no. 20, pp. 3101–3121, 2008, doi: 10.1002/ejic.200800352.
- [11] S. V. Larionov, "Spin transition in iron(III) and iron(II) complexes," *Russian Journal of Coordination Chemistry/Koordinatsionnaya Khimiya*, vol. 34, no. 4, pp. 237–250, 2008, doi: 10.1134/S1070328408040015.
- [12] A. H. Ewald, R. L. Martin, I. G. Ross, A. H. P. R. S. L. White, and S. A., "Anomalous behaviour at the 6 A 1 -2 T 2 crossover in iron (III) complexes," *Proceedings of the Royal Society*



- of London. Series A. Mathematical and Physical Sciences, vol. 280, no. 1381. pp. 235–257, 1964. doi: 10.1098/rspa.1964.0143.
- [13] P. Gu, “2.32 Electronic Spin Crossover ”, vol. 0, no. ii, pp. 421–426.
- [14] P. Gütllich, Y. Garcia, and H. A. Goodwin, “Spin crossover phenomena in Fe(II) complexes,” *Chem. Soc. Rev.*, vol. 29, no. 6, pp. 419–427, 2000, doi: 10.1039/b003504l.
- [15] Y. Garcia and P. Gütllich, “Thermal Spin Crossover in Mn(II), Mn(III), Cr(II) and Co(III) Coordination Compounds,” pp. 49–62, 2012, doi: 10.1007/b95412.
- [16] S. Venkataramani, U. Jana, M. Dommaschk, F. D. Sönnichsen, F. Tuczek, and R. Herges, “Magnetic bistability of molecules in homogeneous solution at room temperature,” *Science (80-. )*, vol. 331, no. 6016, pp. 445–448, 2011, doi: 10.1126/science.1201180.
- [17] J. L. Howe, *Inorganic Chemistry*, 2nd ed., vol. 4, no. 92. Oxford, Melbourne, Tokyo: Oxford University Press, 1896. doi: 10.1126/science.4.92.492-a.
- [18] P. Gütllich, A. B. Gaspar, and Y. Garcia, “Spin state switching in iron coordination compounds,” *Beilstein J. Org. Chem.*, vol. 9, pp. 342–391, 2013, doi: 10.3762/bjoc.9.39.
- [19] S. F. Matar, P. Guionneau, and G. Chastanet, “Multiscale experimental and theoretical investigations of spin crossover FeII complexes: Examples of [Fe (phen) 2 (NCS) 2] and [Fe (PM-BiA) 2 (NCS) 2],” *Int. J. Mol. Sci.*, vol. 16, no. 2, pp. 4007–4027, 2015.
- [20] L. Kreutzburg, C. G. Hübner, and H. Paulsen, “Cooperativity of spin crossover complexes: Combining periodic density functional calculations and Monte Carlo simulations,” *Materials*, vol. 10, no. 2. p. 172, 2017. doi: 10.3390/ma10020172.
- [21] J. Cirera and E. Ruiz, “Computational Modeling of Transition Temperatures in Spin-Crossover Systems,” *Comments Inorg. Chem.*, vol. 39, no. 4, pp. 216–241, 2019, doi: 10.1080/02603594.2019.1608967.
- [22] S. Kajikawa and A. Muraoka, “Theoretical study of the Fe(btr)<sub>2</sub>(NCS)<sub>2</sub> spin-crossover complex with reparameterized density functionals,” *Chem. Phys. Lett.*, vol. 738, no. October 2019, p. 136867, 2020, doi: 10.1016/j.cplett.2019.136867.
- [23] Y. Zhang, “Surface effects on temperature-driven spin crossover in Fe(phen)<sub>2</sub>(NCS)<sub>2</sub>,” *J. Chem. Phys.*, vol. 153, no. 13, 2020, doi: 10.1063/5.0027641.
- [24] G. Brehm, M. Reiher, and S. Schneider, “Estimation of the vibrational contribution to the entropy change associated with the low- to high-spin transition in Fe(phen)<sub>2</sub>(NCS)<sub>2</sub> complexes: Results obtained by IR and Raman spectroscopy and DFT calculations,” *J. Phys. Chem. A*, vol. 106, no. 50, pp. 12024–12034, 2002, doi: 10.1021/jp026586o.
- [25] A. Bousseksou, H. Constant-Machado, and F. Varret, “A Simple Ising-Like Model for Spin Conversion Including Molecular Vibrations,” *J. Phys. I*, vol. 5, no. 6, pp. 747–760, 1995, doi: 10.1051/jp1:1995165.
- [26] A. Bousseksou et al., “Raman spectroscopy of the high-and low-spin states of the spin crossover complex Fe (phen) 2 (NCS) 2: an initial approach to estimation of vibrational contributions to the associated entropy change,” *Chem. Phys. Lett.*, vol. 318, no. 4–5, pp. 409–416, 2000.
- [27] M. Sorai, “Phonon coupled cooperative low-spin 1A<sub>1</sub>high-spin 5T<sub>2</sub> transition in [Fe (phen) 2 (NCS) 2] and [Fe (phen) 2 (NCSe) 2] crystals,” vol. 35, pp. 555–570, 1974.
- [28] H. S. Philipp Gutlich,\* Andreas Hauser and T. Tagawa, “Thermal and Optical Switching of Iron(II) Complexes,” *J. Chem. Eng. Japan*, vol. 44, no. 9, pp. 649–652, 2011, doi: 10.1252/jcej.11we083.
- [29] C. Jury, “Spatiotemporal study of Spin-Crossover materials : Electro-elastic Modelling in bistable,” 2021.
- [30] A. Tissot, “Commutation thermo- et photo-induite de solides moléculaires a transition de spin : du monocristal aux nano-objets To cite this



- version : HAL Id : tel-00665234 UFR Scientifique d'Orsay Ecole doctorale de Chimie de Paris-Sud DOCTEUR EN SCIENCES DE L'UNIVERSITE PARIS XI MOLECULAIRES A TRANSITION DE SPIN : DU MONOCRISTAL AUX NANO-OBJETS," 2012.
- [31] K. Takahashi, Spin-Crossover Complexes. MDPI, 2018. doi: 10.3390/books978-3-03842-826-8.
- [32] F. de L. F. dos S. Martins, "Magnetic properties of first-row transition metal compounds with different nuclearities," 2018.
- [33] J. F. Létard et al., "Critical temperature of the LIESST effect in iron(II) spin crossover compounds," Chem. Phys. Lett., vol. 313, no. 1–2, pp. 115–120, 1999, doi: 10.1016/S0009-2614(99)01036-2.
- [34] G. Molnár et al., "Vibrational spectroscopy of cyanide-bridged, iron(II) spin-crossover coordination polymers: Estimation of vibrational contributions to the entropy change associated with the spin transition," J. Phys. Chem. B, vol. 106, no. 38, pp. 9701–9707, 2002, doi: 10.1021/jp025678a.
- [35] T. Nakamoto, Z. C. Tan, and M. Sorai, "Heat capacity of the spin crossover complex [Fe(2-pic)3]Cl2·MeOH: A spin crossover phenomenon with weak cooperativity in the solid state," Inorg. Chem., vol. 40, no. 15, pp. 3805–3809, 2001, doi: 10.1021/ic010073z.
- [36] P. Guionneau et al., "Structural approach of the features of the spin crossover transition in iron (II) compounds," J. Mater. Chem., vol. 9, no. 4, pp. 985–994, 1999, doi: 10.1039/a808075e.
- [37] C. P. Slichter and H. G. Drickamer, "Pressure-induced electronic changes in compounds of iron," J. Chem. Phys., vol. 56, no. 5, pp. 2142–2160, 1972, doi: 10.1063/1.1677511.
- [38] M. Marchivie, "Approche structurale du phénomène de transition de spin par diffraction des rayons X sous contraintes (T, P, hv) Mathieu," Université Sciences et Technologies - Bordeaux I, 2005. [Online]. Available: tel-00008265 , version 1
- [39] J. Pavlik and R. Boča, "Established static models of spin crossover," Eur. J. Inorg. Chem., no. 5–6, pp. 697–709, 2013, doi: 10.1002/ejic.201201082.
- [40] P. Sambasiva Rao, P. Ganguli, and B. R. McGARVEY, "Proton NMR Study of the High-Spin-Low-Spin Transition in Fe(phen)2(NCS)2 and Fe(pic)3Cl2.(EtOH or MeOH)," Inorg. Chem., vol. 20, no. 11, pp. 3682–3688, 1981, doi: 10.1021/ic50225a020.